

Supporting Information

The HRDC domain oppositely modulates the unwinding activity of *E. coli* RecQ helicase on duplex DNA and G-quadruplex

Fang-Yuan Teng^{1,2,3}, Ting-Ting Wang¹, Hai-Lei Guo¹, Ben-Ge Xin¹, Bo Sun⁴, Shuo-Xing Dou⁵,
Xu-Guang Xi^{1,6,*}, and Xi-Miao Hou^{1,*}

¹State Key Laboratory of Crop Stress Biology for Arid Areas and College of Life Sciences, Northwest A&F University, Yangling, Shaanxi 712100, China

²Experimental Medicine Center, The Affiliated Hospital of Southwest Medical University, Luzhou, Sichuan 646000, China

³ Department of Endocrinology and Metabolism, and Cardiovascular and Metabolic Diseases Key Laboratory of Luzhou, and Sichuan Clinical Research Center for Nephropathy, and Academician (Expert) Workstation of Sichuan Province, The Affiliated Hospital of Southwest Medical University, Luzhou, Sichuan 646000, China

⁴School of Life Science and Technology, ShanghaiTech University, Shanghai, 201210, China

⁵Beijing National Laboratory for Condensed Matter Physics and Laboratory of Soft Matter Physics, Institute of Physics, Chinese Academy of Sciences, Beijing 100190, China

⁶LBPA, Ecole Normale Supérieure Paris-Saclay, CNRS, 4, avenue des Sciences, F-91190 Gif-sur-Yvette, France

*Corresponding author: Xi-Miao Hou. Tel: +86 29 87081664; Fax: +86 29 87081664; Email: houximiao@nwsuaf.edu.cn

And Corresponding author: Xu-Guang Xi. Tel: +33 1 4740 7754; Fax: +33 1 4740 7754; Email: xxi01@ens-cachan.fr

Running title: The function of the HRDC domain in *E. coli* RecQ

Keywords: DNA repair; *E. coli*; RecQ; G-quadruplex; Helicase; Unwinding; Single-molecule

Supplementary Figures

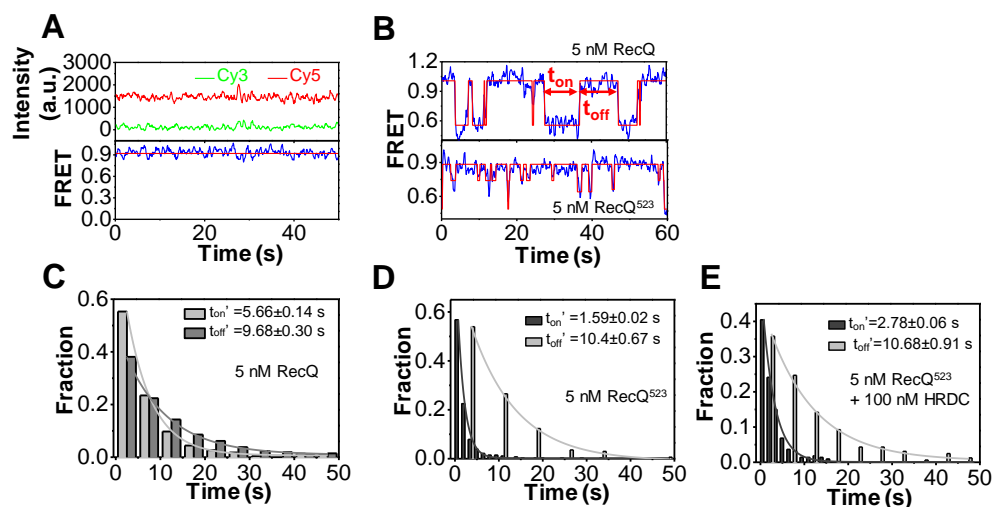


Figure S1. HRDC domain reinforces RecQ binding on the partial duplex by inhibiting its dissociation. (A) In the absence of protein, the fluorescence intensity (upper panel) and corresponding FRET traces (lower panel) of 16bp 12nt-1 are stable, with the FRET efficiency ~ 0.9 . (B) The FRET trace of 16bp 12nt-1 in the presence of 5 nM RecQ or 5 nM RecQ⁵²³. (C-E) Distributions of t_{on} and t_{off} in the traces of 16bp 12nt-1 in 5 nM RecQ, 5 nM RecQ⁵²³, and a mixture of 5 nM RecQ and 100 nM HRDC. t_{on} and t_{off} were measured for more than 200 traces, and the time constants t_{on}' and t_{off}' were generated by the single-exponential fitting.

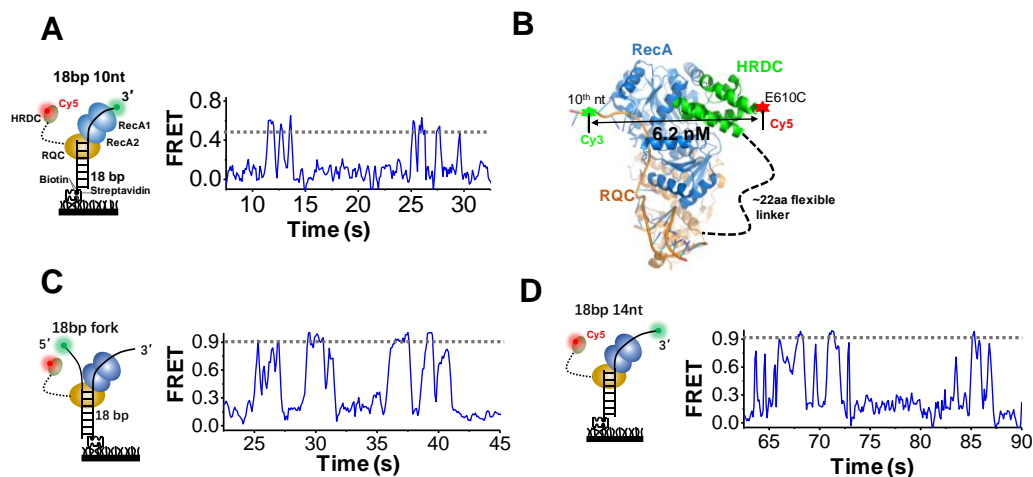


Figure S2. Directly detection of the interaction sites of the HRDC domain. (A) Schematic representation of 18bp 10nt DNA, and the typical trace of the DNA in Cy5-RecQ. A.u. denotes arbitrary unit. In all the following figures, the fluorescence intensities are in arbitrary unit. (B) The rough predicted structure of *E. coli* RecQ in complex with a partial duplex DNA. The crystal structures of *E. coli* RecQ (PDB ID 1OYW), *E. coli* RecQ HRDC (1WUD), *C. sakazakii* RecQ (4TMU), and human BLM (4O3M and 4CGZ) were overlapped in PyMol. The C-terminal of the HRDC domain was ~ 6.2 nm away from the end of the 3'-overhang (10th nucleotide base). (C) Schematic representation of 18bp fork DNA, and the typical FRET trace in 1 nM Cy5-RecQ. (D) The typical traces of 18bp 14nt DNA in 1 nM Cy5-RecQ.

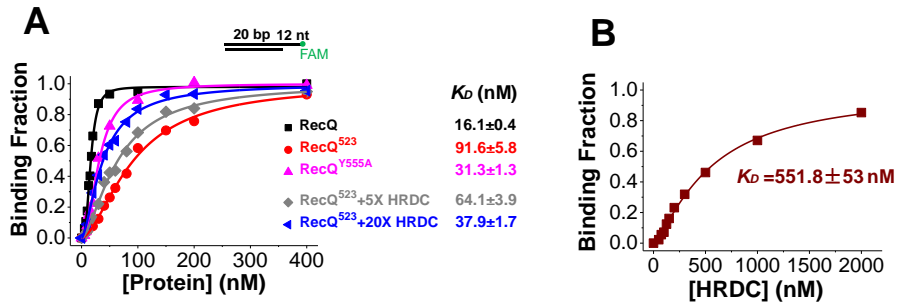


Figure S3. Equilibrium DNA binding assay of RecQ constructs by fluorescence polarization measurement. The binding buffer containing 2 mM MgCl₂, 1 mM DTT, 0.1 mg/mL BSA, and 50 mM KCl in 20 mM Tris-HCl, pH 7.5 was used. The binding curves were fitted by Hill equation $y = [\text{protein}]^n / (K_D^n + [\text{protein}]^n)$, where y is binding fraction, n is Hill coefficient, and K_D is the apparent dissociation constant. (A) Deletion or mutation of the HRDC domain significantly decreases the binding affinity of RecQ on the DNA; however, compensation of 5-, or 20-fold HRDC in RecQ⁵²³ can restore the binding activity to some extent. The Hill coefficients for RecQ, RecQ^{Y555A}, and RecQ⁵²³ are 3.0, 2.1, and 1.7, respectively. When 5-, or 20-fold HRDC are added to RecQ⁵²³, the Hill coefficients are both 1.6 which have little change from that of the RecQ⁵²³ alone. The Hill coefficients reflect that wild-type RecQ binds to DNA with high cooperativity; however, when HRDC is deleted, the cooperativity between individual RecQ molecules is decreased. The free HRDC in solution increases the binding affinity between RecQ⁵²³ and DNA; however, the cooperativity has no obvious change. All these evidence suggest that HRDC may be able to mediate the cooperativity between different RecQ molecules in DNA binding, possibly by dynamically interacting with the core of another RecQ nearby. (B) The HRDC domain binds very poorly to the 20bp 12nt substrate.

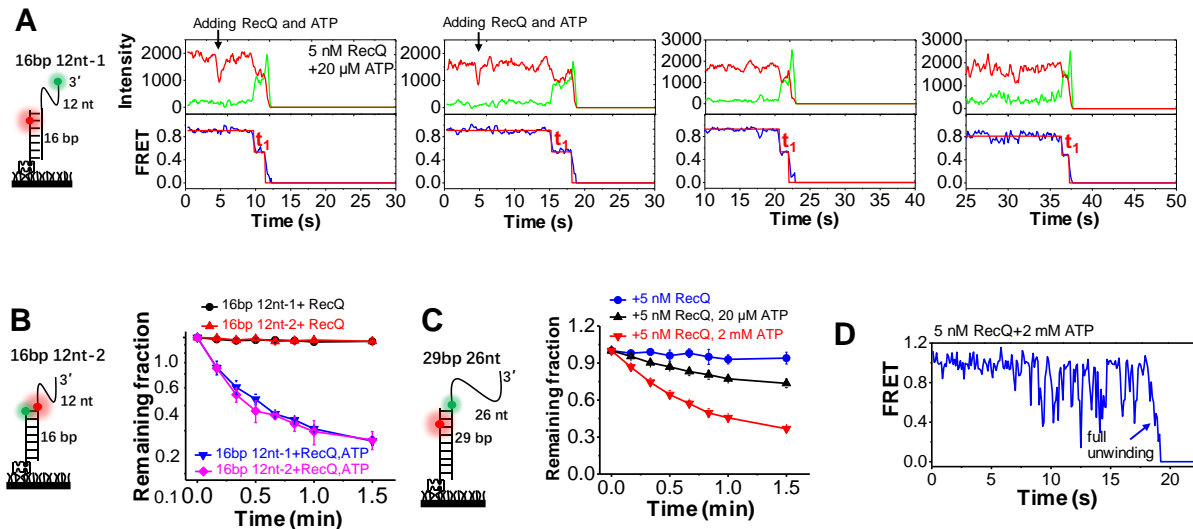


Figure S4. Unwinding of duplex DNA by RecQ. (A) The typical fluorescence and FRET traces of 16bp 12nt-1 in 5 nM RecQ and 20 μ M ATP. (B) Fractions of remaining 16bp 12nt-1 and 16bp 12nt-2 molecules on coverslip *versus* time after addition of 5 nM RecQ and 20 μ M ATP. Lines are the simple connections of the individual data points by Origin 8.0. (C) Fractions of remaining 29bp 26nt molecules on coverslip *versus* time after addition of 5 nM RecQ and 20 μ M ATP or 2 mM ATP. (D) Repetitive unwinding occurred in 29bp 26nt before the final complete unwinding.

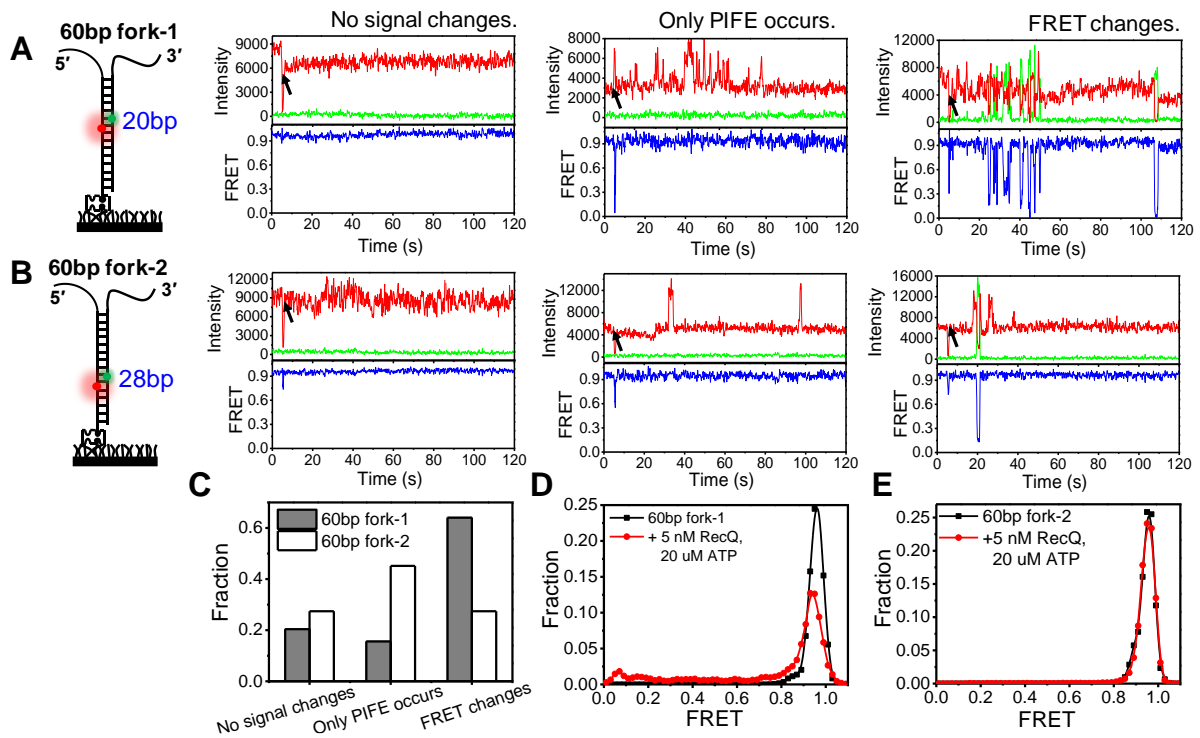


Figure S5. Unwinding of 60 bp fork DNA by RecQ. (A) In 60bp fork-1, Cy3 was labeled in the translocation strand at 20 bp from the junction, and Cy5 was in the displaced strand at 24 bp from the junction. (B) In 60bp fork-2, Cy3 was labeled in the translocation strand at 28 bp from the junction, and Cy5 was in the displaced strand at 32 bp from the junction. Upon the addition of 5 nM RecQ and 20 μ M ATP indicated by the black arrow, three types of FRET traces can be observed in both DNA substrates. In the first type, there is no signal change. In the second type, there are only PIFE (protein-induced fluorescence enhancement) in Cy5, indicating the approaching of Cy5 by RecQ; however, the duplex DNA ahead was not separated. In the third type, PIFE is accompanied by FRET change, suggesting that RecQ not only approaches the Cy5 but also continues to unwind the duplex ahead. (C) The fractions of different types of traces in the two DNA substrates. (D-E) The FRET distribution of 60bp fork-1 and 60bp fork-2 in 5 nM RecQ and 20 μ M ATP. The 60bp fork-1 displays a left shift with a broad range of populations at lower FRET values in RecQ, indicating the unwinding of duplex DNA deeper than 20 bp. The FRET distribution of 60 bp fork-2 does not show obvious change, due to the rare unwinding of duplex DNA deeper than 28 bp.

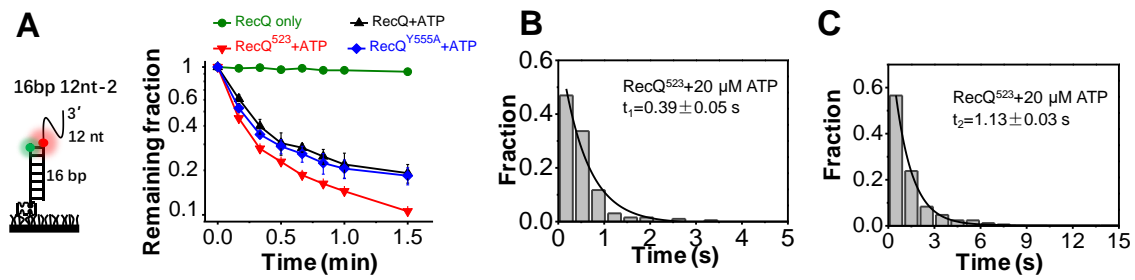


Figure S6. The deletion of HRDC enhances the duplex unwinding activity of RecQ. (A) Fractions of remaining 16bp 12nt-2 molecules on coverslip *versus* time after addition of 5 nM RecQ and 2 mM ATP. Lines are the simple connections of the individual data points by Origin 8.0. (B-C) Distributions of the initiation time t_1 in 16bp 12nt-1, and repetitive unwinding time t_2 in 16bp 12nt-2 in 5 nM RecQ⁵²³.

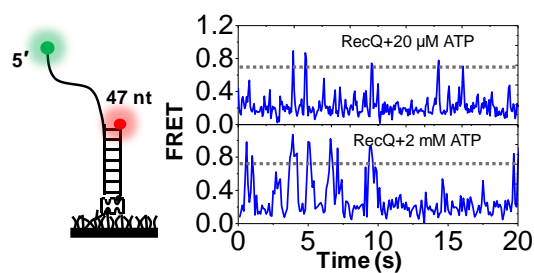


Figure S7. The typical FRET traces of 47nt 17bp at indicated ATP concentrations after removing the excess free RecQ.

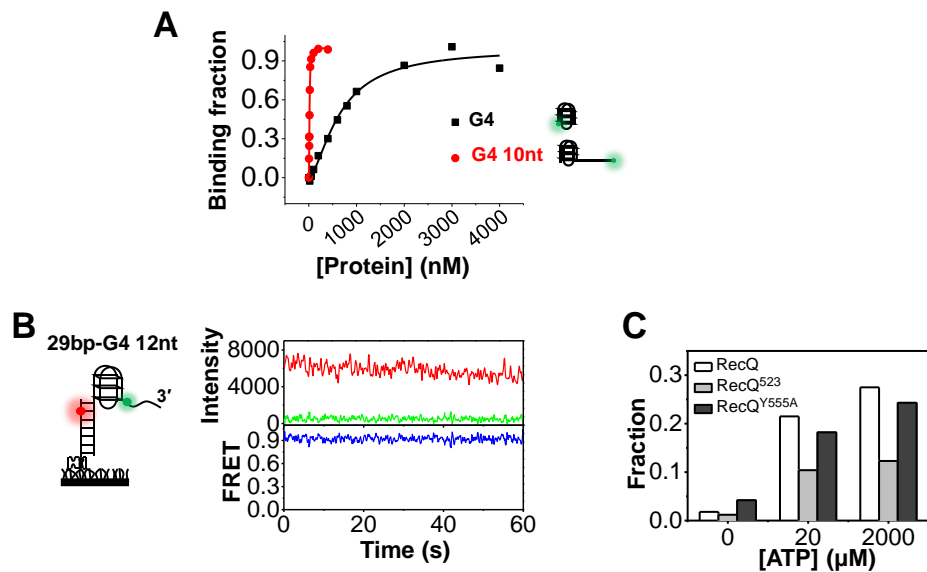


Figure S8. RecQ constructs binding and unwinding G4. (A) RecQ binding to G4 and G4 10nt. The dissociation constant (K_D) of RecQ bound to G4 and G4 10nt are 658.2 ± 79 nM and 15.1 ± 1.1 nM, respectively. (B) The typical trace of 29bp-G4 12nt in 100 mM KCl. (C) The fractions of 29bpG4 12nt with E_{FRET} below 0.65 after adding RecQ constructs and indicated ATP.

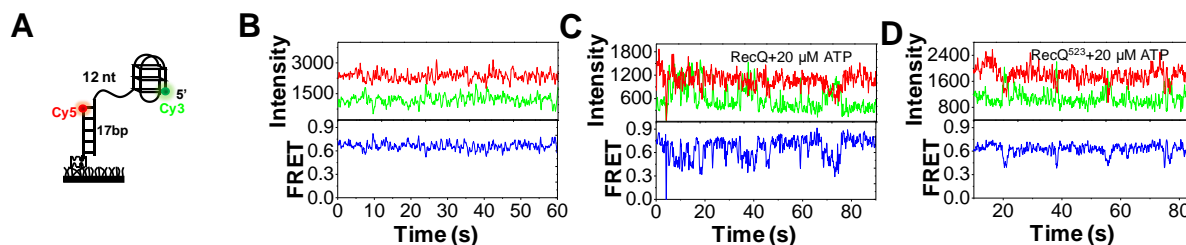


Figure S9. RecQ can unfold the G4 DNA at the 5' end of a partial duplex DNA. (A) Schematic of the G4-containing DNA substrate 17bp 12nt G4. (B) The typical trace of 17bp 12nt G4 in 100 mM KCl. The FRET remains stable with a value of ~ 0.7 . (C) The typical trace of 17bp 12nt G4 in the presence of 5 nM RecQ and 20 μM ATP. (D) The typical trace of 17bp 12nt G4 in the presence of 5 nM RecQ⁵²³ and 20 μM ATP.